

Solar Wind implantation into lunar regolith II: Monte Carlo simulations of hydrogen retention in a surface with defects and the hydrogen (H, H₂) exosphere. O. J. Tucker¹, W. M. Farrell¹, R. M. Killen¹, and D. M. Hurley², ¹NASA Goddard Space Flight Center 8800 Greenbelt Rd., MD 20771, ²John Hopkins University Applied Physics Laboratory 11100 John Hopkins Rd., Laurel, MD 20723.

Introduction: Recently, the near-infrared observations of the OH veneer on the lunar surface by the Moon Mineralogy Mapper (M³) have been refined to constrain the OH content to 500 – 750 parts per million (ppm) [1]. The observations indicate diurnal variations in OH up to 200 ppm possibly linked to warmer surface temperatures at low latitude. We examine the M³ observations using a statistical mechanics approach to model the diffusion of implanted H in the lunar regolith [2, 3]. We present results from Monte Carlo simulations of the diffusion of implanted solar wind H atoms and the subsequently derived H and H₂ exospheres.

Hydrogen Retention: The hydrogen retention model is taken from Farrell et al. (2015, 2017) [2, 3]. The solar wind (SW) flow is composed of density, $n_{sw} = 5 \times 10^6 \text{ H}^+/\text{m}^3$, with velocity $v_{sw} = 400 \text{ km/s}$. The source rate is defined with $n_{sw} v_{sw} \cos(Z)$ where Z is the solar zenith angle. Farrell et al. (2015) [2] demonstrated that the outgassing of hydrogen atoms implanted by the solar wind is more accurately described by considering a distribution of trapped energy values as opposed to a singular value for binding sites within the surface. In this approach, each implanted H atom is given a binding energy U from a Monte Carlo selection of a Gaussian distribution, e. g. $F(U_0, U_w) \sim \exp(-(U - U_0)^2/U_w^2)$, defined by the peak energy U_0 and peak width U_w [2, 3]. The random binding energy sites and local surface temperature are used to define the diffusion time of H to the surface.

Farrell et al. (2017) [3] found that SW hydrogen could be retained in the implantation layer $\sim 22 \text{ nm}$ if there are binding energy sites with energy $U > \sim 0.5 \text{ eV}$ consistent with values derived for irradiated silica and in mature lunar samples. They determined that a Gaussian distribution used to characterize surficial sites with $U_0 = 0.5 \text{ eV}$ and $U_w = 0.1 \text{ eV}$ could produce a diurnal modulation of surface concentrations with lower concentrations in warm regions and the highest concentrations in terminator/polar regions [3]. We refer to this as the nominal case.

We build upon the Farrell et al. studies by performing Monte Carlo simulations of hydrogen in the lunar environment to make quantitative comparisons to the M³ observations. For example, in Figure 1 we show results of simulated surface concentrations for an emissive, nominal and retentive surface each defined by $U_0 = 0.3, 0.5, 0.7 \text{ eV}$,

respectively. For the nominal case, we obtained a quasi-steady state after 2 lunations. At low latitudes the influx is balanced by outgassing, however there is continual buildup of densities near the poles that resulted in a total mass of $\sim 2 \times 10^9 \text{ g}$ over 9 lunations.

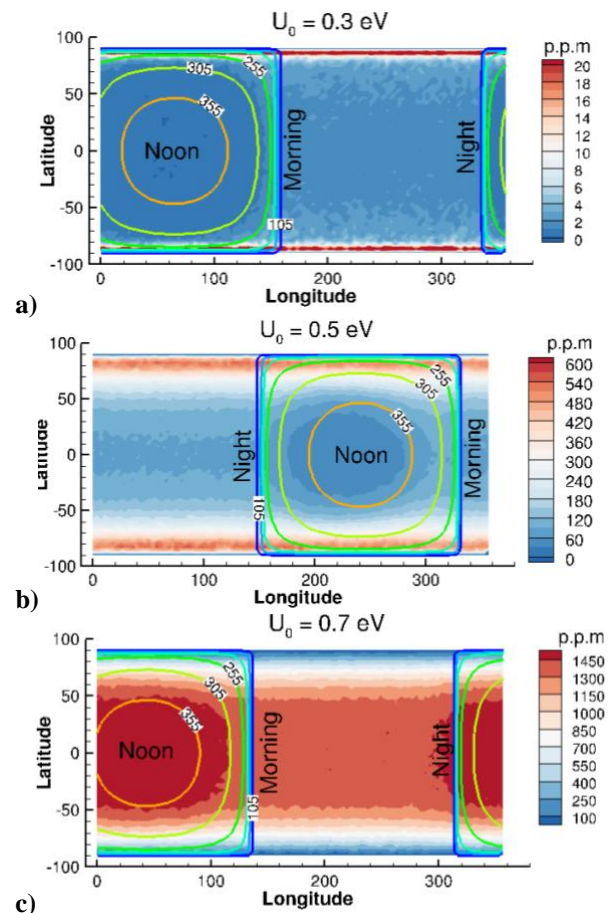


Figure 1: Plots of OH surface concentration for $U_0 = 0.3$ (a), 0.5 (b) and 0.7 (c) eV. The colored lines indicate the local surface temperature [4].

The simulation test cases are used to examine the effect of diffusion on outgassing and the resulting net surface concentration, e.g. $D = D_0 \exp(-U/T)$ [5]. For large values of U atomic mobility is limited at all latitudes, and the surface concentration reflects the SW source. For small values the atoms readily diffuse at low latitudes (highest T), and the concentration increases at higher latitudes where the regolith is cooler. This is also shown in the latitudinal

concentration profiles in Figure 2. It is seen that the nominal test case agrees favorably with the M³ observations especially at latitudes $> \sim 40^\circ$.

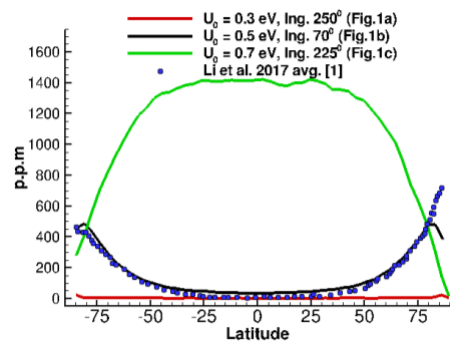
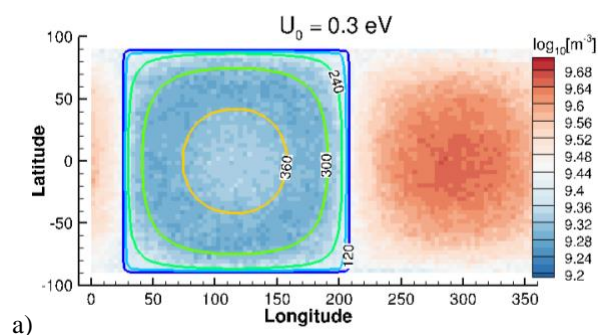
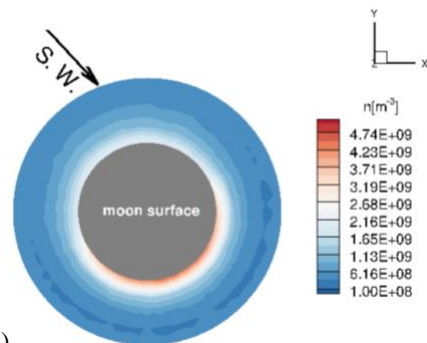


Figure 2: Surface concentration vs. latitude. We compare the modeled surface concentration local midnight (corresponding longitudinal coordinate in the legend) for each simulation case plotted with the averaged M³ observations. Here we assume all implanted H atoms convert to OH. The mass fraction is calculated assuming a regolith density of 1600 kg/m³.

Exospheric Model: The exosphere is model simulates the ballistic trajectories of H and H₂ using a collisionless Monte Carlo approach. The molecules are tracked on a spherical grid including the lunar gravity. The model includes surface residence and photodestruction times for H and H₂ and molecular escape. We consider exospheric distributions populated by thermally accommodated H and H₂. We will compare our results with the Hurley et al. 2016 study on the contribution of solar wind and micrometeoroids to the lunar hydrogen exosphere [6].



a)



b)

Figure 2: a) Near surface H₂ exospheric densities plotted with contour lines of the local surface temperature. b) H₂ exospheric densities in the equatorial out to 2 lunar radii.

In Figure 3 we show preliminary results of the exospheric H₂ densities obtained with the emissive surface test case of $U_0 = 0.3$ eV. Similar to the Hurley et al. 2017 [6] study for a thermal source of H₂ we obtain a modest increase density on the night hemisphere compared to the day hemisphere. Molecules experience lower thermal hops on the night side resulting in a near surface density difference of approximately a factor of 2. However, on the dayside the H₂ molecules have a larger scale height producing an asymmetric cloud about the moon.

Summary: We have applied the implantation code in Farrell et al. (2015, 2017) [2, 3] into a 3D Monte Carlo model the tracks the inventory of implanted h atoms and the subsequent outgassing and exospheric hydrogen cloud. With this new approach, we find that characterizing the lunar surface by a Gaussian distribution of binding energies with $U_0 \sim 0.5$ eV and $U_w \sim 0.1$ eV produces surface concentrations consistent with the M³ observations.

Acknowledgements: This work is supported by the NASA Postdoctoral Program (URSA).

References: [1] Li S. and Milliken R. E. (2017) *Sci. Adv.*, 3:e1701471. [2] Farrell W. M. et al. (2015) *Icarus*, 255, 116 – 126. [3] Farrell W. M. et al. (2017) *J. Geophys. Res. Planets*, 233, 269 – 289. [4] Hurley D. M. et al. (2015) *Icarus*, 255, 159 – 163. [5] Sarukhina, L. V. (2006) *Adv. Space Res.* 37, 50–58 [6] Hurley D. M. et al. (2016) *Icarus*, 000, 1 – 7.